

# SELF-CALIBRATION FOR AIR-BEARING ROTARY ENCODERS

Xiaodong Lu<sup>1</sup>, and David L. Trumper<sup>2</sup>

<sup>1</sup>Dept. of Mechanical Engineering, UBC, Vancouver, BC, Canada

<sup>2</sup>Dept. of Mechanical Engineering, MIT, Cambridge, MA, USA

## INTRODUCTION

High-accuracy rotary encoders are required for rotational axis position measurement in ultra-precision manufacturing and measurement equipments. A typical rotary encoder is made of a glass disk with a fine grating pattern and a scanning read head unit. Digital pulse trains are output from the read head to represent the disk rotary position. The angular measurement accuracy of such a rotary encoder is highly dependent on the grating pattern manufacturing error (uniformity and eccentricity of the graduation), glass disk installation on the measured rotary axis, the scanning head alignment, and signal processing circuits. All these elements unavoidably contribute to rotary encoder errors. If repeatable components of rotary encoder errors can be calibrated accurately, then they can be corrected through software mapping. Calibration of a rotary encoder needs to be conducted after the encoder is installed on the spindle end product, because this installation process may contribute to a significant amount of encoder errors. Therefore, a simple and accurate calibration method is highly desired by end users. Most existing calibration methods are based on a secondary angle sensor of higher accuracy mounted on the same rotary axis as the encoder to be calibrated. Usually that secondary angle sensor installation and setup relies on sophisticated instrument to ensure accuracy [1], and thus cannot be easily performed by end users. Self-calibration encoders have been developed to eliminate the use of a secondary angle sensor for calibration. Watanabe *et al* has demonstrated a self-calibration encoder using five identical read heads evenly distributed around a single optical disk [2]. However, that specially constructed encoder cannot calibrate error components in the 5<sup>th</sup> order spindle rotation frequencies and its harmonics. Moreover, the calibration accuracy also depends on the accuracy of these read heads installation and alignment. Most importantly, this calibration method cannot be applied to most existing encoders.

This work presents the principle, analysis, and experimental results of a novel self-calibration method for rotary encoders on air-bearing supported spindles. By recording the time of each encoder signal edge during spindle free response, calibration curve can be derived by processing the recorded data. Two distinctive features of this method are: 1) it does not need a secondary sensor as a calibration reference; 2) it can be applied to commercial rotary encoders without hardware modification. The experimental results indicate that the calibration repeatability is within 0.002 RMS grating line of the encoder.

Next, we will use our experimental setup as an example to illustrate the self-calibration method and discuss experimental results. The spindle is a Professional Instrument 4R Twin-mount motorized air-bearing spindle. Due to the lack of a high pressure air supply, the air-pressure of the spindle in the calibration process is 80 psi, instead of manufacture recommended 150 psi. A Heidenhain bearing-less optical encoder (ERO 1324-004-2500) is installed on the back of the spindle: the encoder optical disk is on the spindle rotor and the read head unit is on the spindle housing. The optical disk has 2500 grating lines.

## ENCODER SIGNAL PROCESSING

As shown in Fig. 1, the encoder outputs are a pair of quadrature digital signals A/B (2500 pulse/rev) and an index signal (1 pulse/rev). Their rising/falling edges corresponds to N=10,000 spatial sampling events in each revolution to label the spindle rotary position. Essentially these sampling events are evenly spaced in spindle angle domain. The nominal spatial distance between two consecutive sampling events is  $\Delta_0=0.25$  line, where one line corresponds to 1/2500 revolution or 518.4 arc-sec. These events are numbered with reference to the rising edge of the index signal. The encoder error of the k-th sampling event is defined as

$$E(k) = \sum_{i=1}^k \Delta(i) - k\Delta_0, \quad (1)$$

where  $\Delta(i)$  is the actual sampling interval between  $i$ -th and  $(i-1)$ -th event. The time span associated with  $\Delta(i)$  is denoted as  $T(i)$ , which is captured by a circuit of 100 MHz clock. Based on this time measurement, the encoder error will be derived.

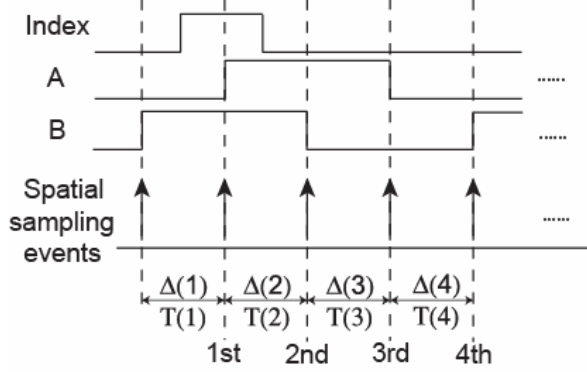


FIGURE 1. Spatial sampling events associated with encoder signals. Signal A, B, and Index are outputs from the rotary encoder. Sampling events are numbered according to the rising edge of the Index pulse.

### ZERO-ORDER METHOD

The most straight-forward way to self-calibrate rotary encoder is to maintain the spindle at perfect constant speed, then the sample intervals can be derived from  $T(i)$  measurement as  $\Delta(k) = \omega_0 T(k)$ , where  $\omega_0$  is the spindle speed and can be calculated as:

$$\omega_0 = \frac{\sum_{k=1}^N \Delta(k)}{\sum_{k=1}^N T(k)} = \frac{N\Delta_0}{\sum_{k=1}^N T(k)}. \quad (2)$$

However, it is impractical to control the spindle speed at a constant speed accurate enough for calibration purpose, due to motor driving torque ripples and feedback sensor errors.

### AIR-BEARING SPINDLE FREE RESPONSE

We propose methods to calibrate the encoder at spindle free response. The spindle is accelerated to a certain speed, and then the spindle motor is turned off, letting the spindle slows down freely. The dynamics equation of the spindle in this free response is

$$I \frac{d\omega}{dt} + C \frac{d\theta}{dt} = 0, \quad \text{where } \theta \text{ is the spindle angle, } I \text{ is the inertia, and } C \text{ is the damping constant. Equivalently in angle domain, we have:}$$

$$\frac{d\omega}{d\theta} = -\frac{C}{I}. \quad (3)$$

Although speed  $\omega$  is not a linear function of time, it is a linear function of angle  $\theta$  and thus the spindle speed at  $k$ -th sampling event  $\omega(k) = \Delta(k)/T(k)$  is a linear function of sampling event index  $k$ . This is the basis of our self-calibration method. As the actual value of  $\Delta(k)$  is not known yet, from time measurement  $T(k)$  we can calculate apparent spindle speed  $\omega_b(k) = \Delta_0/T(k)$  using the nominal value of  $\Delta(k)$ . This apparent speed is the combination of the spindle speed and encoder error:  $\omega_b(k) = \omega(k) + (\Delta_0 - \Delta(k))/T(k)$ . Fig. 2 shows an experimentally measured spindle apparent speed. By estimating the linear component  $\omega(k)$  from measurement  $\omega_b(k)$ , encoder grating spacing  $\Delta(k)$  can be calibrated using the first-order method derived in the next section.

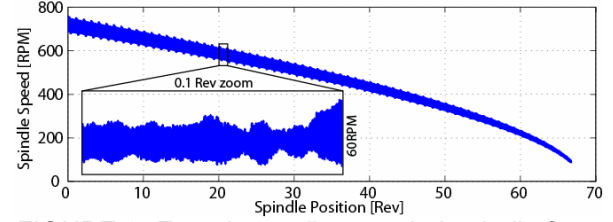


FIGURE 2. Experimentally recorded spindle free response versus spindle rotation over 65 revolutions. The insert shows the detailed apparent speed waveform within 0.1 revolution.

### FIRST-ORDER SELF-CALIBRATION METHOD

Assuming the spindle damping is a constant, from Equation (3) the spindle speed can be parameterized as  $\omega(k) = \omega_0 + a \times k$ , where  $\omega_0$  and  $a$  are unknown constants to be estimated. The spatial interval is expressed as:

$$\Delta(k) = T(k) \times (\omega_0 + a \times k). \quad (4)$$

Summing the data together over a full recorded revolution starting from the  $s$ -th sampling event, we have

$$\sum_{i=s+1}^{s+N} \Delta(i) = \sum_{i=s+1}^{s+N} T(i) \times (\omega_0 + a \times i), \quad (5)$$

where  $s$  is the starting point of the data batch over one full revolution. The left side is exactly one revolution:

$$N \times \Delta_0 = \omega_0 \times \sum_{i=s+1}^{s+N} T(i) + a \times \sum_{i=s+1}^{s+N} T(i) \times i. \quad (6)$$

Combining (4) and (6), we get

$$\Delta(k) = T(k) \times \frac{N \times \Delta_0}{\sum_{i=s+1}^{s+N} T(i)} + a \times \left( k - \frac{\sum_{i=s+1}^{s+N} T(i) \times i}{\sum_{i=s+1}^{s+N} T(i)} \right) \times T(k) \equiv F(a, k) \quad (7)$$

$$k = s + 1, \dots, s + N.$$

However, this equation is not sufficient to estimate parameter  $a$ . Two batches of data are used as shown in Fig. 3 with starting point  $s_1$  and  $s_2 (> s_1)$ , and parameter  $a_1$  and  $a_2$ , respectively. Applying Equation (7) to both data batches, we have  $2N$  equations:

$$\begin{aligned} \Delta(k) &= F_1(a_1, k), \quad k = s_1 + 1, \dots, s_1 + N; \\ \Delta(k) &= F_2(a_2, k), \quad k = s_2 + 1, \dots, s_2 + N. \end{aligned} \quad (8)$$

Canceling out  $\Delta(k)$  in Equation (8), we get

$$\begin{cases} F_1(a_1, k) = F_2(a_2, k + N), \text{ for } k = s_1 + 1, \dots, s_2 \\ F_1(a_1, k) = F_2(a_2, k), \text{ for } k = s_2 + 1, \dots, s_1 + N \end{cases} \quad (9)$$

Note, Equation (9) consists of  $N$  equations, and each of them is a linear function of two unknown parameters  $a_1$  and  $a_2$ . Through least square fitting, we can get the best estimate of these parameters  $\bar{a}_1$  and  $\bar{a}_2$ . Plugging  $a_1 = \bar{a}_1$  back to Equation (8), we can get the calibration of sample interval  $\Delta(k)$  for  $k = 1, \dots, N$ .

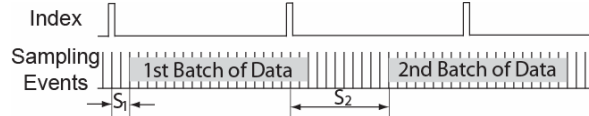


FIGURE 3. Phase relation of two batches of data for self-calibration.

### EXPERIMENTAL CALIBRATION RESULTS

Applying this self-calibration algorithm to the experimental data in Fig. 2, Fig. 4 shows the calibrated grating error  $\Delta(k) - \Delta_0$  at 700 RPM speed. The starting points of the two batches of data used are  $s_1=0$  and  $s_2=5000$ , corresponding to 180 deg phase shift. Integrating this grating error according to Equation (1), the resulting encoder error is plotted in Fig. 5.

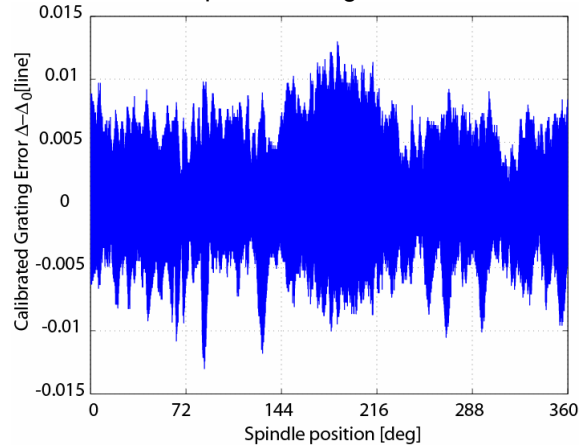


FIGURE 4. Calibrated encoder grating error. 700 rpm spindle speed,  $s_1=0$ , and  $s_2=5000$ .

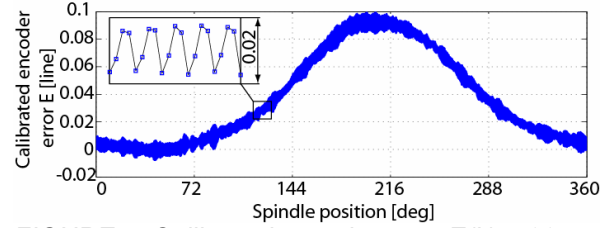


FIGURE 5. Calibrated encoder error  $E(k)$ . 700 rpm spindle speed,  $s_1=0$ , and  $s_2=5000$ . The insert shows a detailed view of the encoder error.

Fig. 5 shows that this encoder has a maximum error of 0.11 grating lines. The insert indicates that significant error comes from the misalignment of two detectors for signal A and B. In spatial frequency domain, the Fourier Transform of this encoder error is shown in Fig. 6. The amplitude of the encoder error decodes with the increase of spatial frequency, however, at 2500 and 5000 cycles/rev the detector misalignment error increases significantly.

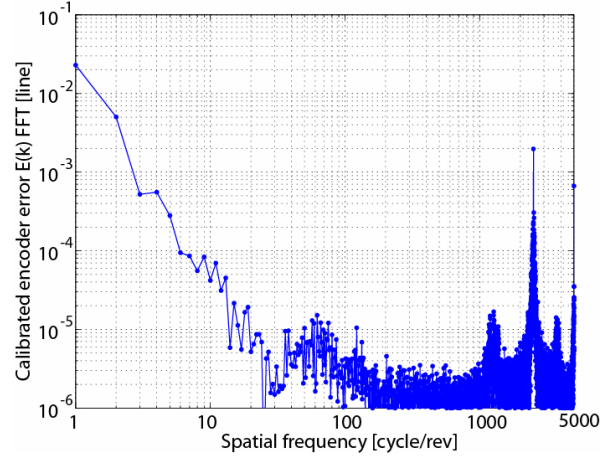


FIGURE 6. FFT of calibrated encoder error  $E(k)$ . 700 rpm spindle speed,  $s_1=0$ , and  $s_2=5000$

In order to evaluate the above calibration results, we investigated the repeatability of the calibration results at various spindle speeds and starting points of data batches.

### REPEATABILITY VS DATA PHASE SHIFT

First, at 700RPM and fixing  $s_1=0$ , we applied the first-order algorithm on the same experimental data in Fig. 2 with different  $s_2$ . The calibrated encoder error map with  $s_2=5000$  is used as a reference  $E_0(k)$ , and calibrated map with other  $s_2$  is  $E(k, s_2)$ . The calibration repeatability  $R(s_2)$  is the root mean square of the difference between two maps:  $E_0(k)$  and  $E(k, s_2)$

$$R(s_2) = \sqrt{\frac{\sum_{k=1}^{10000} (E(k, s_2) - E_0(k))^2}{10000}}. \quad (10)$$

Fig. 7 shows this repeatability as a function of the phase shifts of two data batch  $s_2 - s_1$ . This result indicates that the calibration repeatability is less than 0.002 grating line for most phase shift. However, when the phase shift of two data batches is close to 0 or 10000 samples (equivalent to 0 or 360 deg of spindle rotation), the repeatability degrades significantly due to singularity of Equation (9). To ensure accurate calibration result, the phase shift of two batches should be selected between 90 and 270 deg of rotation.

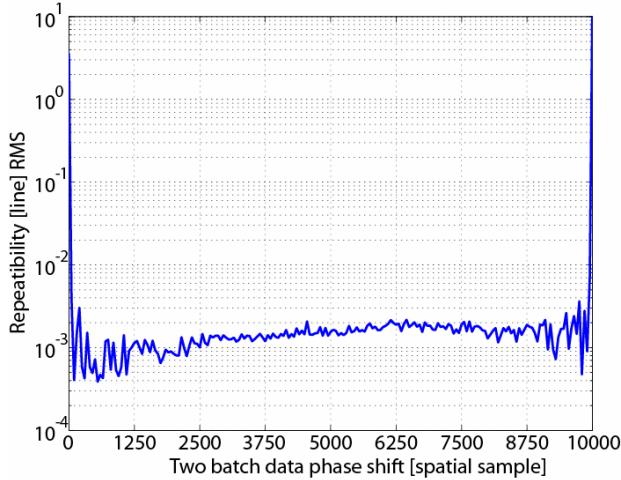


FIGURE 7. Calibration repeatability versus phase shift of two data batches. The spindle speed is 700 RPM.

#### REPEATABILITY VS SPINDLE SPEED

Applying the first order self-calibration algorithm to the whole data in Fig. 2 by fixing  $s_1=0$  and  $s_2=5000$ , we investigated calibration repeatability versus spindle speed. The calibrated encoder error map at 700 RPM is used as a reference  $E_0(k)$  and the calibrated map at speed  $n$  is  $E(k, n)$ . The calibration repeatability  $R(n)$  is the root mean square of the difference between two maps  $E_0(k)$  and  $E(k, n)$ :

$$R(n) = \sqrt{\frac{\sum_{k=1}^{10000} (E(k, n) - E_0(k))^2}{10000}}. \quad (11)$$

The dashed line in Fig. 8 shows this repeatability of the first-order self-calibration method as a function of the spindle speed. This result indicates the repeatability degrades as the spindle speed decrease. This is caused by the nonlinear damping of the spindle air bearing. From Fig. 2, it is obvious that the spindle damping increases as speed slows down over a

large speed range. Actually, the damping of the spindle also changes even within one revolution, and thus deviates from the constant damping assumption used in first-order algorithm.

To improve the calibration repeatability, we further developed the second order algorithm, which assumes the damping coefficient to change linearly with spindle speed and thus the spindle speed can be parameterized as:

$$\omega(k) = \omega_0 + a \times k + b \times k^2, \quad (12)$$

where  $a$  and  $b$  are unknown parameters to be estimated. The mathematics of the second order self-calibration method can be derived in a similar way to the first order method. Applying second-order method to the experimental data in Fig 2, the calibration repeatability versus speed is shown by the solid line of Fig. 8. Much better than that of first-order method, the repeatability of second-order method is less than 0.002 grating line for speed range from 300 RPM to 700 RPM. Therefore, the calibration error map obtained from this speed range should be used. Once the error map is established, it can be used at any spindle speed. Through this calibration, the rotary encoder accuracy is enhanced from 0.12 lines to 0.002 lines RMS.

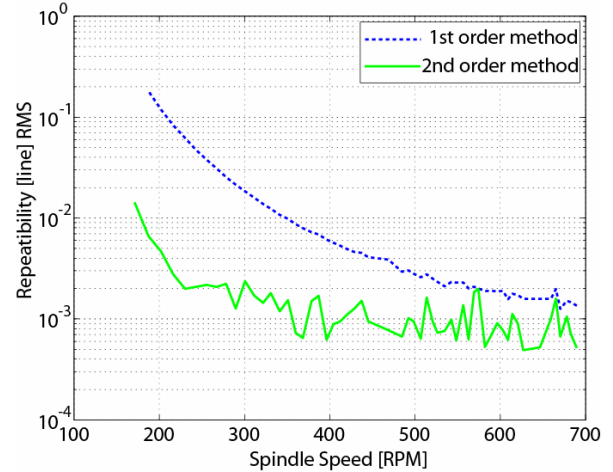


FIGURE 8. Calibration repeatability versus spindle speed. The calibration map of 700 RPM is used as a reference.  $s_1=0$ , and  $s_2=5000$ .

#### REFERENCES

1. Satoshi Kiyono *et al*, 1997, Self-calibration of precision angle sensor and polygon mirror, Measurement, Vol 21, No 4, pp125-136.
2. Tsukasa Watanabe *et al*, 2005, Self-Calibration Rotary Encoder, 7<sup>th</sup> International Symposium on Measurement Technology and Intelligent Instruments, Journal of Physics: Conference Series 13 (2005) pp 240-245.